Hindawi
Shock and Vibration
Volume 2019, Article ID 4207473, 10 pages
https://doi.org/10.1155/2019/4207473

Research Article

Load Localization and Reconstruction Using a Variable Separation Method

Jing Zhang, Fang Zhang, and Jinhui Jiang

State Key Laboratory of Mechanics and Control of Mechanical Structures, Nanjing University of Aeronautics and Astronautics, Nanjing, China

Correspondence should be addressed to Fang Zhang; zhangfangyy@163.com

Received 27 February 2019; Accepted 19 March 2019; Published 1 April 2019

Academic Editor: Marco Tarabini

Load identification is very important in engineering practice. In this paper, a novel method for load reconstruction and localization is proposed. In the traditional load localization method, location information is coupled to the impulse response matrix. The inversion of the impulse response matrix leads the process of load localization to be time-consuming. So we propose a variable separation method to separate the load location information from the impulse response matrix. An error optimization function of load histories in different modes is employed to determine the true load location. After locating the external load, the load time history can be easily reconstructed by the measurement responses and determinate impulse response matrix. This method is verified by simulations of a simply supported beam acted by a sine load and an impact separately. An experiment is also carried out to validate the feasibility and accuracy of the proposed method.

1. Introduction

Knowledge of external loads and load locations is crucial in various fields, such as structural dynamic design, noise reduction, and fault diagnosis. However, it is usually difficult to directly measure the structure external loads and the locations due to some physical or economical limitations. This is why indirect methods must be developed to identify structural loads by using measured structural responses, such as acceleration, velocity, displacement, and strain.

In recent years, with the deepening of the research on structure dynamics, the techniques of load identification have developed rapidly. Currently, there are two mature methods of load identification: frequency-domain methods and time-domain methods. The frequency-domain method converts the kinetic equation into linear equation in the frequency domain. Bartlett and Flannelly [1] firstly used the frequency-domain methods to identify the hub forces in a helicopter model. Starkey and Merrill [2] used direct inversion of the frequency response function (FRF) to determine the load. In their research, they found the frequency response function (FRF) was ill-posed near the resonance zone, and with the number of the loads increasing, the accuracy of the identification result was reduced. Doyle [3] established a waveguide model to describe the dynamic response and employed the spectral analysis to reconstruct the impacting force acting on a two-dimensional bimaterial beam system. Liu and Shepard [4] used enhanced least squares schemes to reduce the random errors of structural response signals. In their researches, a total least squares scheme was also employed to solve the errors associated with the FRF matrix. The applications of the frequency-domain methods are often restricted since sufficient long data are required to apply the Fourier transformation or other harmonic transformation which is often used in frequency-domain methods. Thus, the time-domain method of load identification was developed. The research of time-domain methods started relatively late and still has many problems need to be solved. Desanghere and Snoeys [5] established the time-domain method of load identification and firstly used the modal coordinate transformation to identify the external load. Chang and Sun [6] employed a deconvolution method to reconstruct the time history of structure loads. The load identification is an inverse problem, where the structural

properties and responses are known while the external loads need to be determined. However, this inverse problem is mathematically ill-posed in most case, which means that the uniqueness and the stability of the solution are lost. A little noise in the measured responses of the structure, which is inevitable, would result in the great change of the estimated load. To solve this ill-posed problem, some regularization techniques are introduced to stabilize the identified load. Jacquelin et al. [7] compared the efficiency of two widely used regularization techniques, the Tikhonov method and the truncated singular value decomposition (TSVD), by identifying an impact acting on a circular Kirchhoff plate. In their research, they also compared the effect of two-parameter choice criterion, L-curve method, and generalized cross validation (GCV). Besides these two methods, there are also some commonly used regularization methods, such as the modified TSVD [8], the damped singular value decomposition [9], and the iterative regularization methods [10]. Liu et al. [11, 12] introduced several new regularization filter function and confirmed the effectiveness and the accuracy of proposed methods for solving load identification problems. In many researches including those mentioned above, the main purpose is to reconstruct the time history of the excitation and the load location is assumed as known information, which is often not the case and needs to be identified before the reconstruction of load time history. In fact, the process of load identification consists of two separate parts: localization of the external load and reconstruction of the load time history. In order to identify the load location, wavelets were introduced to locate the external loads. Gaul and Hurlebaus [13] employed the wavelet transform to determine the arrival time of impact wave to different sensors and used an optimization method to identify the impact location. As for impact load, there are several localization methods by analyzing wave propagation, such as time difference of arrival (TDOA) [14, 15], direction of arrival (DOA) [16, 17], and wave's energy loss with traveled distance [18, 19]. Ginsberg and Fritzen [20] created a sample-force-dictionary as the prior knowledge to transform the impact identification into a sparse recovery task. Li and Lu [21] adopted a complex method to determine the location of the impact and then identify the impact history by using a constrained optimization scheme. They [22] used a two-step iterative approach to both localize and reconstruct a single point force acting on a structure. In their research, they proposed the stabilization diagram of identified locations to determine the appropriate regularization range and the true force location. However, these two studies have the same problem: the location information is coupled to the impulse response matrix, which generally needs to be inverted in the process of load identification. Thus, to identify the load position, a considerable amount of matrix inversion is needed and a lot of time will be consumed.

In this paper, a new localization method is proposed, which separates the location variable from the impulse response matrix. In this method, a modal decomposition method is adopted and only once matrix inversion needs to be done to obtain several-order modal force. The load position is identified by optimizing an error function of the modal force. Numerical simulation and identification test on a simply supported beam structure are implemented to demonstrate the accuracy and effectiveness of the proposed method. This paper is organized as follows: in Section 2, the inverse model for load localization and reconstruction is discussed, with introducing regularization techniques. The applied method for fast localization is also proposed. In Section 3, both numerical simulation and experiment are carried out to validate the proposed method. Finally, concluding remarks are presented in Section 4.

2. Load Localization and Reconstruction Scheme

2.1. Inverse Model. First, we construct the relationship between a concentrated force and responses of a structure. Without loss of generality, a multiple degree-of-freedom system is considered as the structure model, and the degree of freedom of the system is assumed as N. Generally, the dynamic equilibrium equation of the MDOF system is expressed as

$$\mathbf{M}\ddot{u}(t) + \mathbf{C}\dot{u}(t) + \mathbf{K}\mathbf{u}(t) = \mathbf{P}(t), \tag{1}$$

where $\mathbf{M}$, $\mathbf{C}$, and $\mathbf{K}$ represent the mass, damping, and stiffness matrixes, respectively. $\mathbf{u}(t)$ is the response vector of the system, and $\mathbf{P}(t)$ is the external load vector.

Under the zero initial condition, the relation between the responses and the load can be written as the form of a convolution:

$$\mathbf{u}(t) = \mathbf{h}(t) * \mathbf{P}(t), \tag{2}$$

where $\mathbf{h}(t)$ is the unit impulse response matrix, and it can be expressed through the following modal superposition:

$$\mathbf{h}(t) = \sum_{r=1}^{N} \frac{\boldsymbol{\varphi}_r \boldsymbol{\varphi}_r^T}{m_r \omega_r \sqrt{1-\xi_r^2}} e^{-\xi_r \omega_r t} \sin\sqrt{1-\xi_r^2}\,\omega_r t, \tag{3}$$

where m_r, ξ_r, and ω_r are the rth-order modal mass, damping ratio, and natural circular frequency, respectively. $\boldsymbol{\varphi}_r$ is the rth-order mode of vibration.

For a concentrated force, s_f is assumed as the load location, and $f(t)$ is the load time history. The response of the ith degree of freedom is obtained:

$$u_i(t) = \int_0^t \sum_{r=1}^{N} h_r(t-\tau)\varphi_r(i)\varphi_r(s_f) f(\tau) d\tau, \tag{4}$$

where $h_r(t)$ is the rth-order impulse response function:

$$h_r = \frac{1}{m_r \omega_r \sqrt{1-\xi_r^2}} e^{-\xi_r \omega_r t} \sin\sqrt{1-\xi_r^2}\,\omega_r t. \tag{5}$$

The summation part in equation (4) can be represented by

$$h_{i,s_f}(t) = \sum_{r=1}^{N} h_r(t)\varphi_r(i)\varphi_r(s_f). \tag{6}$$

The subscript of $h_{i,s_f}(t)$ denotes the ith DOF unit impulse response with load acting on the location s_f. The convolution in equation (4) can be taken into a discrete form:

$$\begin{bmatrix} u_i(t_1) \\ u_i(t_2) \\ \vdots \\ u_i(t_Q) \end{bmatrix} = \begin{bmatrix} h_{i,s_f}(t_1) & 0 & \cdots & 0 \\ h_{i,s_f}(t_2) & h_{i,s_f}(t_1) & \cdots & 0 \\ \vdots & \vdots & \ddots & \vdots \\ h_{i,s_f}(t_Q) & h_{i,s_f}(t_{Q-1}) & \cdots & h_{i,s_f}(t_1) \end{bmatrix} \begin{bmatrix} f(t_0) \\ f(t_1) \\ \vdots \\ f(t_{Q-1}) \end{bmatrix} \Delta t, \tag{7}$$

where Δt denotes the sampling interval, Q denotes the number of sampling points, and $t_i = i\Delta t\,(i = 0, 1, 2, \ldots, Q)$. Equation (7) can be simplified as

$$\mathbf{u}_i = \mathbf{H}(i, s_f) \cdot \mathbf{f}. \tag{8}$$

For a certain system, the only unknown variables in equation (8) are the load location s_f and load time history $\mathbf{f}$. To determine the location s_f, two or more measurement points are chosen to obtain corresponding load time history $\mathbf{f}$. A minimum optimization problem is established to find the suitable value of location s_f, which makes the error function value of several load vectors $\mathbf{f}$ minimum. In this process, there are lots of matrix inversion because the location variable s_f is included in the matrix $\mathbf{H}$. Generally, the size of the matrix $\mathbf{H}$ is large, due to the number of sampling points Q. Thus, the process of load localization will cost plenty of time which may cause unknown problems during researches and practical engineering situations.

2.2. New Load Localization Method. To reduce the time of load localization, a new method is considered which separates the load location s_f from the matrix $\mathbf{H}$. In this method, the number of matrix inversions is reduced significantly so that the load location can be identified faster.

From equation (6), $h_{i,s_f}(t)$ is expressed as the form of the modal superposition. By substituting equations (6) and (8), the following equation can be derived:

$$\mathbf{u}_i = \sum_{r=1}^{N} \varphi_r(i)\varphi_r(s_f)\mathbf{H}_r \cdot \mathbf{f}, \tag{9}$$

where

$$\mathbf{H}_r = \begin{bmatrix} h_r(t_1) & 0 & \cdots & 0 \\ h_r(t_2) & h_r(t_1) & \cdots & 0 \\ \vdots & \vdots & \ddots & \vdots \\ h_r(t_Q) & h_r(t_{Q-1}) & \cdots & h_r(t_1) \end{bmatrix}. \tag{10}$$

Combining the component $\varphi_r(s_f)$ and load time history $\mathbf{f}$, equation (9) is turned into

$$\mathbf{u}_i = \sum_{r=1}^{N} \varphi_r(i)\mathbf{H}_r \cdot \mathbf{S}_r, \tag{11}$$

where $\mathbf{S}_r = \varphi_r(s_f) \cdot \mathbf{f}\,(r = 0, 1, 2, \ldots, N)$. Then, summation in equation (11) can be transformed to a matrix form:

$$\mathbf{u}_i = \mathbf{W}_i \cdot \mathbf{S}, \tag{12}$$

where

$$\begin{aligned} \mathbf{W}_i &= [\, \varphi_1(i)\mathbf{H}_1 \;\; \varphi_2(i)\mathbf{H}_2 \;\; \cdots \;\; \varphi_N(i)\mathbf{H}_N \,]_{Q\times NQ}, \\ \mathbf{S} &= [\, \mathbf{S}_1 \;\; \mathbf{S}_2 \;\; \cdots \;\; \mathbf{S}_N \,]^T_{1\times NQ}. \end{aligned} \tag{13}$$

From equation (12), we can see that the load location s_f is included in the vector $\mathbf{S}$, and the matrix $\mathbf{W}_i$ only contains the information of measurement point and properties of the system. Thus, the matrix $\mathbf{W}_i$ is defined when the measurement point is settled. However, the vector $\mathbf{S}$ cannot be calculated by directly inversing equation (12) because equation (12) is an undetermined system of equation.

Thus, to obtain the vector $\mathbf{S}$ uniquely, the modal truncation method is employed and the m modes which contribute the most to the response are chosen. Equation (12) is transformed to

$$\mathbf{u}_i = \mathbf{W}_i^{\text{trun}} \cdot \mathbf{S}^{\text{trun}}, \tag{14}$$

where

$$\begin{aligned} \mathbf{W}_i^{\text{trun}} &= [\, \varphi_1(i)\mathbf{H}_1 \;\; \varphi_2(i)\mathbf{H}_2 \;\; \cdots \;\; \varphi_m(i)\mathbf{H}_m \,]_{Q\times mQ}, \\ \mathbf{S}^{\text{trun}} &= [\, \mathbf{S}_1 \;\; \mathbf{S}_2 \;\; \cdots \;\; \mathbf{S}_m \,]^T_{1\times mQ}. \end{aligned} \tag{15}$$

In addition, the responses of other measurement points are necessary. Assuming that responses of m points are known, then we have

$$\mathbf{Y} = \mathbf{W}^{\text{trun}} \cdot \mathbf{S}^{\text{trun}}, \tag{16}$$

where

$$\begin{aligned} \mathbf{Y} &= [\, \mathbf{u}_1^T \;\; \mathbf{u}_2^T \;\; \cdots \;\; \mathbf{u}_m^T \,]^T, \\ \mathbf{W}^{\text{trun}} &= \begin{bmatrix} \varphi_1(1)\mathbf{H}_1 & \varphi_2(1)\mathbf{H}_2 & \cdots & \varphi_m(1)\mathbf{H}_m \\ \varphi_1(2)\mathbf{H}_1 & \varphi_2(2)\mathbf{H}_2 & \cdots & \varphi_m(2)\mathbf{H}_m \\ \vdots & \vdots & \ddots & \vdots \\ \varphi_1(m)\mathbf{H}_1 & \varphi_2(m)\mathbf{H}_2 & \cdots & \varphi_m(m)\mathbf{H}_m \end{bmatrix}. \end{aligned} \tag{17}$$

Equation (16) can be inversed directly because $\mathbf{W}^{\text{trun}}$ is a $mQ \times mQ$ matrix. Then $\mathbf{S}_i\,(i = 1, 2, \ldots, m)$ are calculated, and m load vectors can be obtained:

$$\mathbf{f}_i = \frac{\mathbf{S}_i}{\varphi_i(s_f)}, \quad i = 1, 2, \ldots, m. \tag{18}$$

For the true load location s_f, the m load vectors $\mathbf{f}_i\,(i = 1, 2, \ldots, m)$ are equal. Thus, an optimization function is introduced:

$$\eta(s_f) = \sum_{i=1}^{m} \left\| \mathbf{f}_i - \frac{1}{m} \sum_{r=1}^{m} \mathbf{f}_r \right\|_2. \tag{19}$$

From equation (19), the optimization function $\eta(s_f)$ gets the minimum value when the variable s_f is the true load location. Thus, the load localization is transformed to a minimum optimization problem.

In this method of load localization, only once matrix inversion is computed, which reduces the operation time greatly and increases the efficiency of load localization. For a certain system, the matrix $\mathbf{W}^{\text{trun}}$ is determined when the measurement points, the sampling interval, and the number

of sampling points are all defined. Therefore, the load location can be quickly identified, as the responses are measured by the sensors. In addition, the selection of modes is a very important part in this method. The identified location may not be accurate, if a specific mode is not kept. Thus, the selected modes should reflect the response as far as possible. As the number of selected modes is limited by the number of measurement points, the identified result of a load with a wide range of frequencies would not be effective when the number of measuring points is not large enough. Furthermore, the normalized modal shape values must be measured, which is difficult to realize in the real work. This problem needs to be solved with the help of finite element techniques.

Due to the modal truncation, the load time history which is obtained in this method may not be accurate enough. Thus, after identifying the load location, the load time history can be reconstructed by equation (8).

2.3. Regularization Method. Since the matrix $\mathbf{W}^{\text{trun}}$ is generally ill-posed, the direct inversion of equation (16) would not give a stable result. The identified result is sensitive to the errors including signal sampling errors, modal truncation errors, and rounding errors. A little error will cause the direct inverse solution change a great deal.

Considering the errors, the measurement response can be expressed as

$$\mathbf{Y}_\delta = \mathbf{W}^{\text{trun}} \cdot \mathbf{S}^{\text{trun}} + \boldsymbol{\delta}, \tag{20}$$

where $\boldsymbol{\delta}$ is the error data of responses and $\mathbf{Y}_\delta$ is the measurement response including errors data. The singular value decomposition of $\mathbf{W}^{\text{trun}}$ is

$$\mathbf{W}^{\text{trun}} = \mathbf{U}\boldsymbol{\Omega}\mathbf{V}^T = \sum_{r=1}^{mQ} \mathbf{u}_r \sigma_r \mathbf{v}_r^T, \tag{21}$$

where $\mathbf{U} = [\mathbf{u}_1, \mathbf{u}_2, \ldots, \mathbf{u}_{mQ}]$ and $\mathbf{V} = [\mathbf{v}_1, \mathbf{v}_2, \ldots, \mathbf{v}_{mQ}]$ are matrixes with orthonormal columns and $\boldsymbol{\Omega} = \text{Diag}(\sigma_i)$ $(i = 1, 2, \ldots, mQ)$ has nonnegative diagonal singular values appearing in the nonincreasing order. Thus, equation (20) gives a formulation of the identified result

$$\begin{aligned} \mathbf{S}^* &= \left(\mathbf{W}^{\text{trun}}\right)^{-1} \mathbf{Y}_\delta = \mathbf{V}\text{Diag}\left(\sigma_i^{-1}\right)\mathbf{U}^T\mathbf{Y}_\delta \\ &= \mathbf{S}^{\text{trun}} + \sum_{i=1}^{mQ} \sigma_i^{-1}\left(\mathbf{u}_i^T\boldsymbol{\delta}\right)\mathbf{v}_i. \end{aligned} \tag{22}$$

As shown in equation (22), the ill-posed factor of the load identification model is controlled by using the smaller singular value σ_i rather than the maximal singular value σ_1. With the singular values going down to zero, the error of measurement responses would strongly influence the stability of identified results. To reduce this effect, the regularization method is introduced to filter the small singular values. σ_i^{-1} in equation (22) is coupled with a regularization operator $p(\alpha, \sigma_i)$, and the parameter α can make $p(\alpha, \sigma_i)$ decay to zero when σ_i approaches zero. Thus, the stable identified result can be obtained:

$$\mathbf{S}^* = \mathbf{V}\text{Diag}\left(p(\alpha, \sigma_i)\sigma_i^{-1}\right)\mathbf{U}^T\mathbf{Y}_\delta = \sum_{i=1}^{mQ} p(\alpha, \sigma_i)\sigma_i^{-1}\left(\mathbf{u}_i^T\mathbf{Y}_\delta\right)\mathbf{v}_i. \tag{23}$$

The regularization operator is selected as follows:

$$p(\alpha, \sigma_i) = \frac{\sigma_i^2}{\sigma_i^2 + \alpha}. \tag{24}$$

This regularization method has turned into the famous regularization method called the Tikhonov regularization method. The regularization parameter α is generally determined with a certain criterion, such as L-curve criterion and GCV criterion.

3. Tests and Results

3.1. Numerical Simulation. In this section, two numerical simulations of a simply supported beam model are implemented to verify the proposed method. In this beam model, the length is 1 m long, and the cross section is 6 cm × 1 cm. The material of the beam has the density 7800 kg/m^3, Young's module 210 GPa and Poisson's ratio 0.3. The beam is evenly divided into 1000 elements, and there are 1001 nodes in total. The first two-order natural frequencies of the beam are $f_1 = 23.5$ Hz and $f_2 = 94.1$ Hz. Two displacement sensors are installed at $x_1 = 0.23$ m and $x_2 = 0.45$ m from one simply supported end, and the beam model is excited by a sine load and an impact separately, as shown in Figure 1.

3.1.1. Identification of a Sine Load. The beam is excited by a load $\mathbf{F}_1$, which is shown in Figure 2. $\mathbf{F}_1$ is a sine load with frequency $f = 60$ Hz acting at the point $a_1 = 0.35$ m from one simply supported end. The measurement responses of the two points x_1 and x_2 are computed through the analytical response expression of simply supported beams, and 5% (5% of the maximum of the measured signals) Gaussian white noise has been added to the responses. The responses of the two points are shown in Figures 3 and 4.

To localize the load, the first two-order modes are adopted. There is only one matrix inversion needing to be done in the identification procedure. Furthermore, the Tikhonov regularization method is used to overcome the ill-condition of the matrix inversion.

The regularization parameter α is determined by the L-curve method, which is shown in Figure 5. The red dot indicates the regularization parameter $\alpha = 0.0028$. The two vectors $\mathbf{S}_1$ and $\mathbf{S}_2$ are calculated through equation (23). To identify the true load location, the 999 nodes are assumed as the load location, except the two ends. At each assumed load location, the two load vectors $\mathbf{f}_1$ and $\mathbf{f}_2$ can be obtained by using equation (18) and corresponding optimization function value η is computed. Figure 6 shows the curve of η and the load location with minimum value of η is 0.356 m from one simply supported end, which is very close to the true load location $a_1 = 0.35$ m. $\mathbf{f}_1$ and $\mathbf{f}_2$ in the identified load location are shown in Figure 2. At the same time, the relative

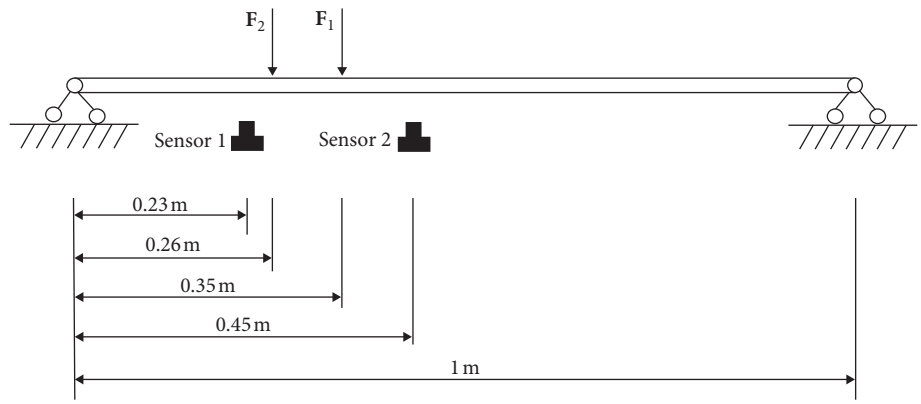

Figure 1: Beam simulation model.

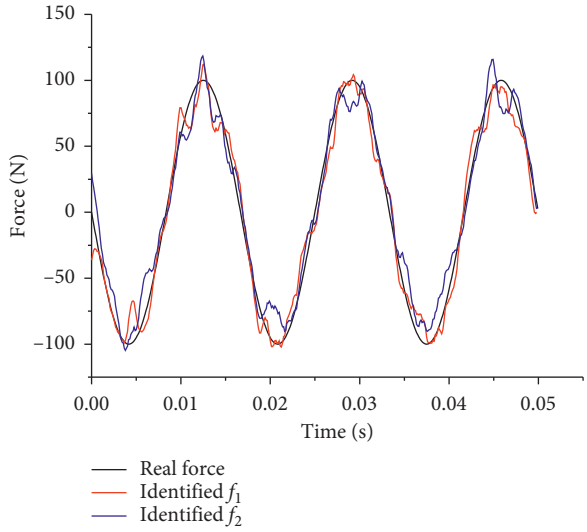

Figure 2: Real load history and identified loads of $\mathbf{F}_1$.

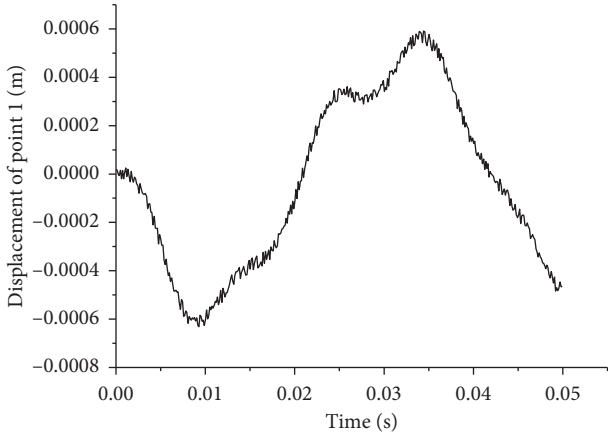

Figure 3: Displacement response of point 1 by $\mathbf{F}_1$.

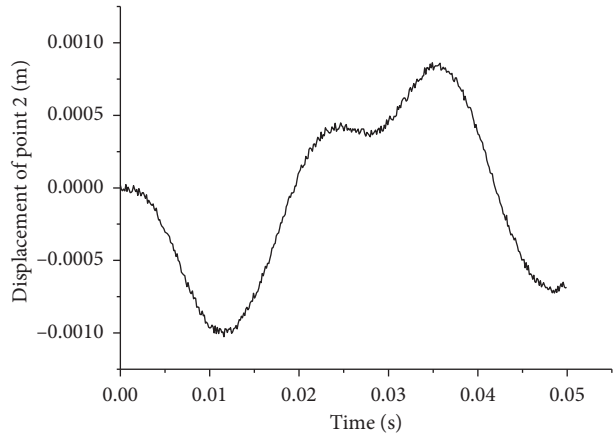

Figure 4: Displacement response of point 2 by $\mathbf{F}_1$.

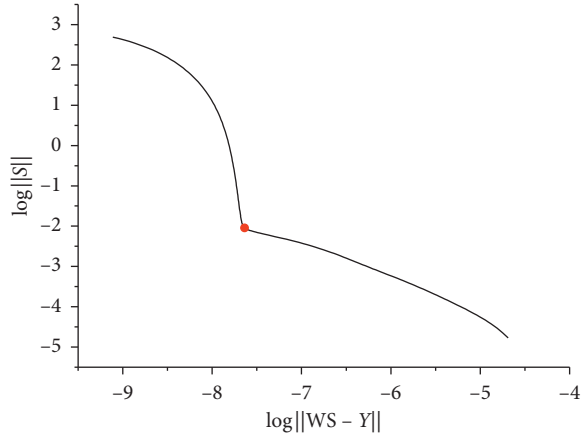

Figure 5: The L-curve plot of $\mathbf{F}_1$.

error and the correlation coefficient of $\mathbf{f}_1$ and $\mathbf{f}_2$ are listed in Table 1.

In Table 1, the identified $\mathbf{f}_1$ and $\mathbf{f}_2$ can be used to describe the external load, but they still have some noticeable oscillatory components. To reconstruct the load history more accurately, the responses of measure points x_1 and x_2 are, respectively, used to identify the load history by regularizing equation (8) as the load location has already been determined. The reconstruction of the load history is shown in Figure 7. The relative error and the correlation coefficient of the reconstruction are listed in Table 1. It can be found that the reconstruction by measurement response of point 2 is closest to the real load. This is because the response value and the SNR (signal-to-noise ratio) of point x_2 are larger to these of point x_1. The final result is considered satisfactory.

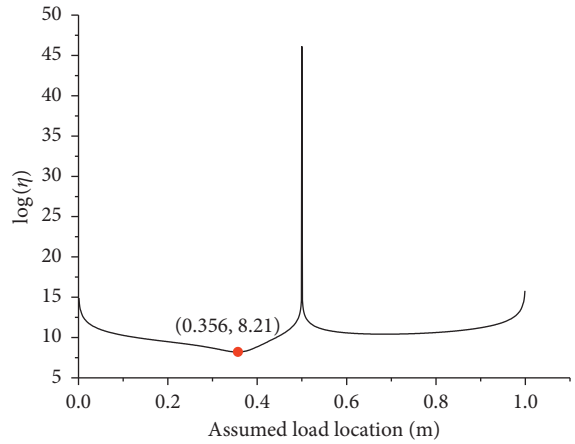

Figure 6: The optimization function value of $\mathbf{F}_1$.

Table 1: The relative error and the correlation coefficient of the identified $\mathbf{F}_1$.

	$\mathbf{f}_1$	$\mathbf{f}_2$	Point x_1	Point x_2
Relative error	0.1599	0.1845	0.231	0.1159
Correlation coefficient	0.9876	0.9876	0.9815	0.9945

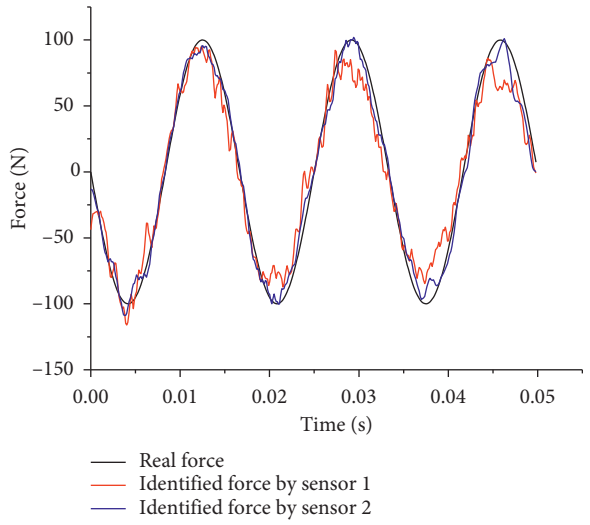

Figure 7: The reconstruction of the load $\mathbf{F}_1$.

3.1.2. Identification of an Impact. In this section, a simulation of the beam excited by using an impact load $\mathbf{F}_2$ is carried out to verify the proposed method. The impact load $\mathbf{F}_2$ is shown in Figure 8, acting at the point $a_2 = 0.26$ m from one simply supported end. The measurement responses of the two points x_1 and x_2 are computed through the analytical response expression of simply supported beams, and 5% (5% of the maximum of the measured signals) Gaussian white noise has been added to responses. The responses of the two points are shown in Figures 9 and 10.

In the same way, the first two-order modes are used to identify the impact location, and the Tikhonov regularization method is employed to reduce the influence of the errors on the identified result. The regularization parameter

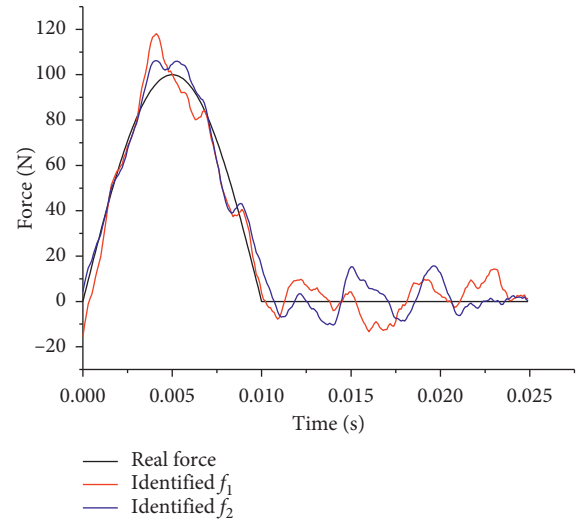

Figure 8: Real load history and identified loads of $\mathbf{F}_2$.

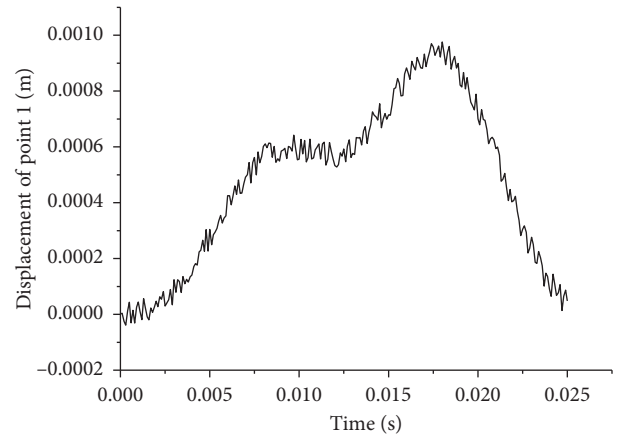

Figure 9: Displacement response of point 1 by $\mathbf{F}_2$.

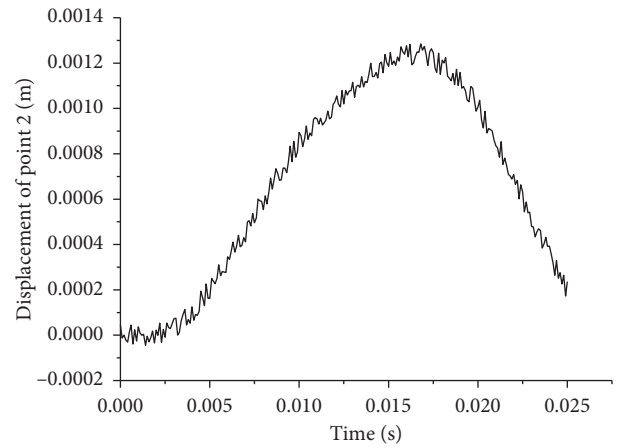

Figure 10: Displacement response of point 2 by $\mathbf{F}_2$.

α is determined by the L-curve method, which is shown in Figure 11. The red dot indicates the regularization parameter $\alpha = 0.0054$.

To localize the impact load, the optimization function value η at each assumed load location is computed, and the curve of η is shown in Figure 12. The identified load location

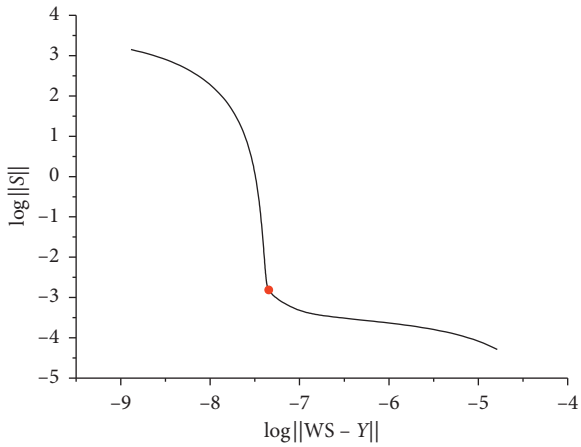

Figure 11: The L-curve plot of $\mathbf{F}_2$.

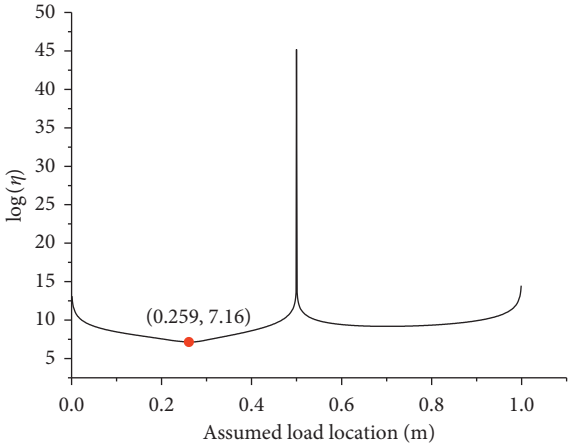

Figure 12: The optimization function value of $\mathbf{F}_2$

is 0.259 m from one simply supported end. This identified result is very close to the actual impact location $a_2 = 0.26$ m. The corresponding $\mathbf{f}_1$ and $\mathbf{f}_2$ in the identified load location are compared in Figure 8. We also use the response of measure point x_2 to reconstruct the impact history, which is shown in Figure 13. The relative error and the correlation coefficient of the reconstruction are listed in Table 2. The reconstruction can describe the external load well, so the identified result is accepted.

3.2. Experiment. For experimental validation of the proposed localization method, an experimental test of a steel simply supported beam was set up. As shown in Figure 14, the steel rectangular beam is simply supported at the two ends and the geometric dimension of this beam is measured. The length, width, and thickness are $l = 0.695$ m, $w = 0.04$ m, and $h = 0.007$ m, respectively. The sensors used in this experiment are two PCB piezoelectric accelerometers and one force transducer of Model Number 208C02. An impact hammer with a rubber head is used to excite the beam, and the sampling frequency is 4096 Hz.

The modal parameters are obtained by the system identification techniques. The experiment values of the first

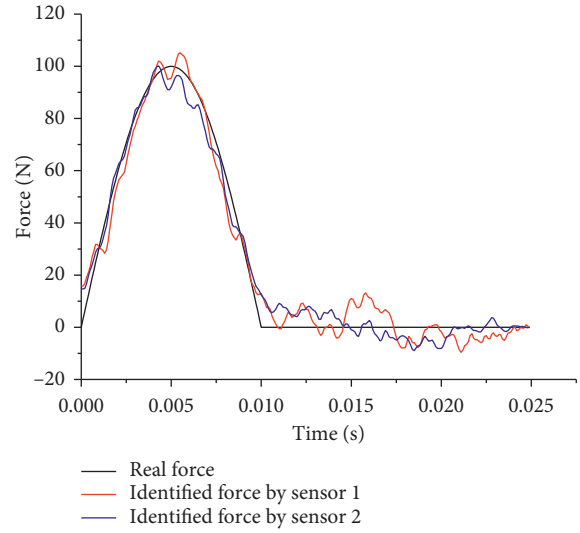

Figure 13: The reconstruction of the impact $\mathbf{F}_2$.

Table 2: The relative error and the correlation coefficient of the identified $\mathbf{F}_2$.

	$\mathbf{f}_1$	$\mathbf{f}_2$	Point x_1	Point x_2
Relative error	0.2051	0.1808	0.1339	0.1138
Correlation coefficient	0.9713	0.9792	0.9867	0.9911

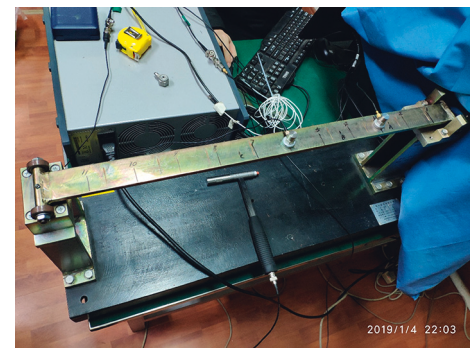

Figure 14: Experimental model of the simply supported beam.

three-order natural frequencies are recorded in Table 3. The experiment values of the first three-order modal damping ratio are $\xi_1 = 0.0026$, $\xi_2 = 0.0013$, and $\xi_3 = 0.0009$. According to the natural frequencies obtained by the experiment, the finite element model of the beam is established and the modal shape values φ can be calculated from this finite element model. The beam is evenly divided into 695 elements, and there are 696 nodes in total. The simulation values of the first three-order natural frequencies are also recorded in Table 3.

Eleven mark points are distributed on the beam, and two accelerometers are installed at points 3 and 6, shown in Figure 14. The beam is impacted at points A, B, and C separately. The real location of these impacts is shown in Table 4. The measurement of the accelerometers is integrated twice to obtain the displacement responses of the measure points. As shown in Figure 15, an FRF analysis shows that

Table 3: Natural frequency of the beam (unit: Hz).

	1st	2nd	3rd
Test	39.37	153.41	346.74
Simulation	38.48	153.91	346.30

Table 4: Identified locations of the experiment.

	A	B	C
True locations (m)	0.15	0.25	0.43
Identified locations (m)	0.151	0.252	0.431
Absolute error (m)	0.001	0.002	0.001

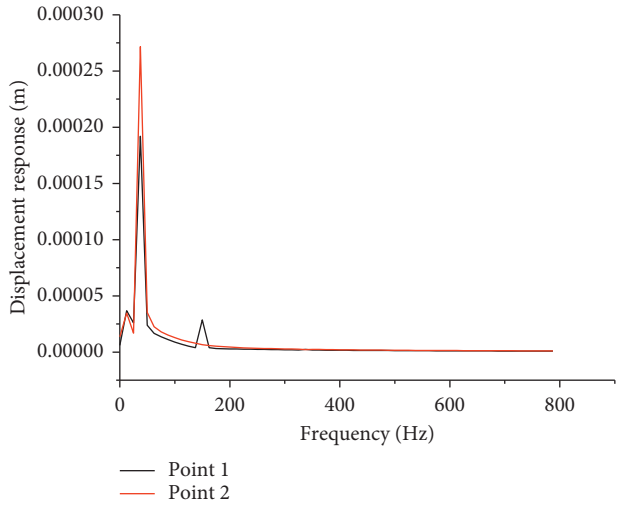

Figure 15: FRF of the displacement responses by impact A.

the displacement responses are mainly involved in the first two modes, which are used to identify the impact location. After computing the optimization function value η at each node, the impact locations are identified and shown in Figures 16–18 separately.

The details of the identified locations are shown in Table 4. It can be seen that the identified locations coincide with the true impact locations well for all three impact points A, B, and C. After determining the impact location, the force histories can be reconstructed. By using the responses of sensor 2 installed at point 6, the comparison of the measured and identified time histories of the three impacts are shown in Figures 19–21, respectively. The relative error and the correlation coefficient of the reconstructions are listed in Table 5. For all three impact test, the identified results have good consistency. Thus, the experiment result is satisfactory and verifies the credibility of the proposed method.

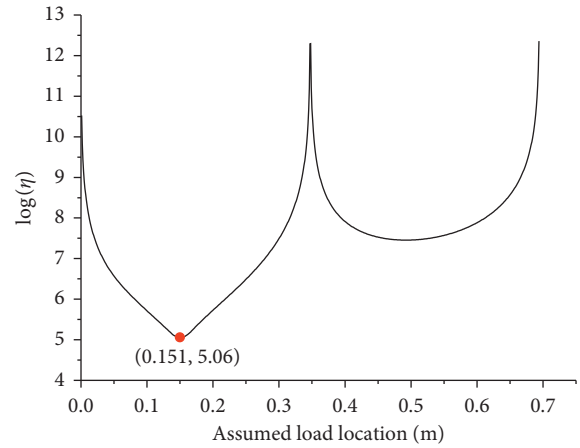

Figure 16: The optimization function value of impact A.

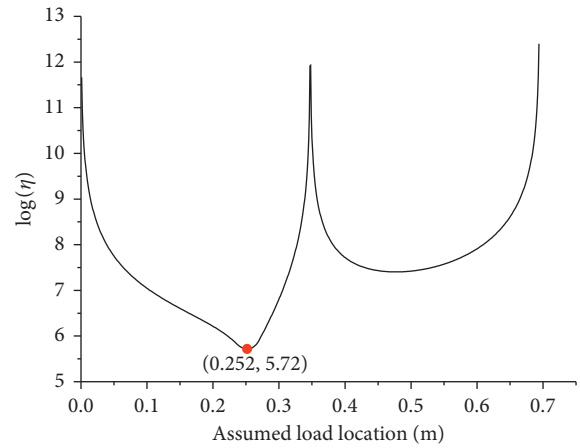

Figure 17: The optimization function value of impact B.

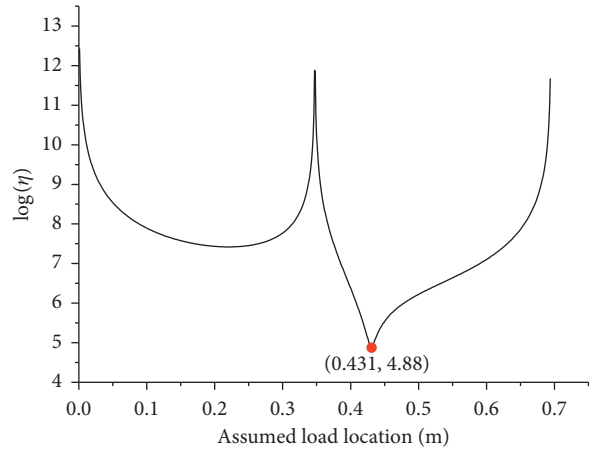

Figure 18: The optimization function value of impact C.

4. Conclusion

In this paper, the problem of load localization and reconstruction from structural responses is addressed. In order to improve the problem that a lot of matrix inversions in the identification process consume much operation time, a variable separation method is proposed. This method separates the load location variable from the impulse response matrix which needs to be inversed in the localization process. We take several order modes in which the response is mainly included and identify the stable time history vectors of the corresponding modes. In this step, there is

Table 5: The relative error and the correlation coefficient of the identified impacts.

	A	B	C
Relative error	0.1440	0.1195	0.1207
Correlation coefficient	0.9943	0.9957	0.9965

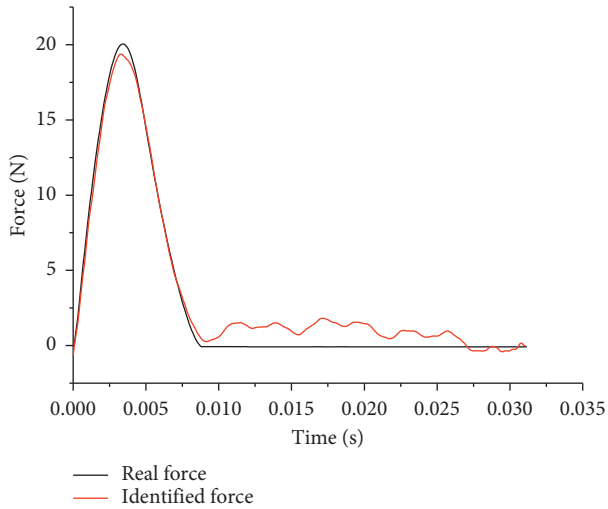

Figure 19: The reconstruction of the impact A.

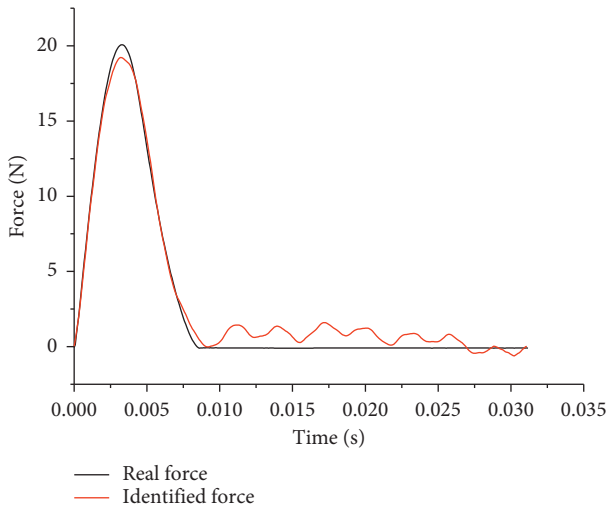

Figure 20: The reconstruction of the impact B.

only once matrix inversion and it can be replaced by singular value decomposition method. The regularization method is employed to overcome the ill-posed problem and obtain the stable time history vector. Then we compute the force history through dividing the time history vector by corresponding mode shape value. The load location is determined with error function using the minimum optimization method. After identifying the location, this problem is transformed into the classic reconstruction of force history. By using the regularization method and L-curve criterion, the force history is inversely computed. The proposed method is fully demonstrated and verified with simulations of a simply supported beam separately acted by a sine load and an impact. An experiment is also implemented to prove the validity of the method.

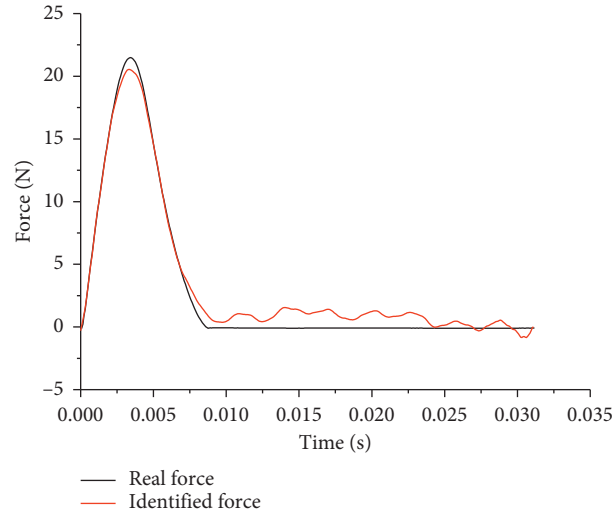

Figure 21: The reconstruction of the impact C.

Data Availability

The simulation and experiment data used to support the findings of this study are included within the supplementary information files.

Conflicts of Interest

The authors declare that they have no conflicts of interest.

Acknowledgments

This work was supported by a project funded by the National Natural Science Foundation of China, no.51775270. Our research was also supported by the Priority Academic Program Development of Jiangsu Higher Education Institution.

Supplementary Materials

The codes and data used in this manuscript are included in the "supplementary information.zip" file. The specific description of the files is listed as follows: Simulation 1: the M file "simulation _sin load.m" is the Matlab code to simulate the identification of a sine load. Simulation 2: the txt files "u1err_sin2d.txt" and "u2err_sin2d.txt" are the responses data of the sine load simulation. Simulation 3: the M file "simulation_impact.m" is the Matlab code to simulate the identification of an impact load. Simulation 4: the txt files "u1err_impact2d.txt" and "u2err_impact2d.txt" are the responses data of the impact load simulation. Experiment 5: the M file "experiment_impactA.m" is the Matlab code to verify the identification of impactA. Experiment 6: the txt files "experiment_impactA_response1.txt" and "experiment_impactA_response2.txt" are the measured responses of the experiment of impactA. Experiment 7: the txt file "experiment_impactA_Force.txt" is the measured data of impactA. Experiment 8: the M file "experiment_impactB.m"

is the Matlab code to verify the identification of impactB. Experiment 9: the txt files "experiment_impactB_response1.txt" and "experiment_impactB_response2.txt" are the measured responses of the experiment of impactB. Experiment 10: the txt file "experiment_impactB_Force.txt" is the measured data of impactB. Experiment 11: the M file "experiment_impactC.m" is the Matlab code to verify the identification of impactC. Experiment 12: the txt files "experiment_impactC_response1.txt" and "experiment_impactC_response2.txt" are the measured responses of the experiment of impactC. 13. The txt file "experiment_impactC_Force.txt" is the measured data of impactC. (*Supplementary Materials*)

References

[1] F. D. Bartlett and W. G. Flannelly, "Model verification of force determination for measuring vibratory loads," *Journal of the American Helicopter Society*, vol. 24, no. 2, pp. 10–18, 1979.

[2] J. M. Starkey and G. L. Merrill, "On the ill-condition nature of indirect force measurement techniques," *International Journal of Analysis and Experimental Modal Analysis*, vol. 4, no. 3, pp. 103–108, 1989.

[3] J. F. Doyle, "Force identification from dynamic responses of a bimaterial beam," *Experimental Mechanics*, vol. 33, no. 1, pp. 64–69, 1993.

[4] Y. Liu and W. S. Shepard, "Dynamic force identification based on enhanced least squares and total least-squares schemes in the frequency domain," *Journal of Sound and Vibration*, vol. 282, no. 1-2, pp. 37–60, 2005.

[5] G. Desanghere and R. Snoeys, "Indirect identification of excitation forces by modal coordinate transformation," in *Proceedings of the 3rd International Modal Analysis Conference (IMAC)*, pp. 685–690, Orlando, FL, USA, January 1985.

[6] C. Chang and C. T. Sun, "Determining transverse impact force on a composite laminate by signal deconvolution," *Experimental Mechanics*, vol. 29, no. 4, pp. 414–419, 1989.

[7] E. Jacquelin, A. Bennani, and P. Hamelin, "Force reconstruction: analysis and regularization of a deconvolution problem," *Journal of Sound and Vibration*, vol. 265, no. 1, pp. 81–107, 2003.

[8] P. C. Hansen, T. Sekii, and H. Shibahashi, "The modified truncated SVD method for regularization in general form," *SIAM Journal on Scientific and Statistical Computing*, vol. 13, no. 5, pp. 1142–1150, 1992.

[9] M. P. Ekstrom and R. L. Rhoads, "On the application of eigenvector expansions to numerical deconvolution," *Journal of Computational Physics*, vol. 14, no. 4, pp. 319–340, 1974.

[10] M. Hanke and P. C. Hansen, "Regularization methods for large-scale problems," *Surveys on Mathematics for Industry*, vol. 3, pp. 253–315, 1993.

[11] L. Wang, X. Han, J. Liu, X. He, and F. Huang, "A new regularization method and application to dynamic load identification problems," *Inverse Problems in Science and Engineering*, vol. 19, no. 6, pp. 765–776, 2011.

[12] X. Sun, J. Liu, X. Han, C. Jiang, and R. Chen, "A new improved regularization method for dynamic load identification," *Inverse Problems in Science and Engineering*, vol. 22, no. 7, pp. 1062–1076, 2014.

[13] L. Gaul and S. Hurlebaus, "Identification of the impact location on a plate using wavelets," *Mechanical Systems and Signal Processing*, vol. 12, no. 6, pp. 783–795, 1998.

[14] A. G. Woolard, A. A. Phoenix, and P. A. Tarazaga, "Assessment of large error time-differences for localization in a plate simulation," in *Dynamics of Coupled Structures*, vol. 4, pp. 369–376, Springer, Cham, Switzerland, 2016.

[15] J. D. Poston, R. M. Buehrer, and P. A. Tarazaga, "Indoor footstep localization from structural dynamics instrumentation," *Mechanical Systems and Signal Processing*, vol. 88, pp. 224–239, 2017.

[16] H. Lee, J. W. Park, and A. Helal, *Estimation of Indoor Physical Activity Level Based on Footstep Vibration Signal Measured by MEMS Accelerometer in Smart Home Environments*, Springer-Verlag, Berlin, Germany, 2009.

[17] S. J. McManus and D. Green, "Continued development of broadband passive bearing estimation," in *Proceedings of the OCEANS'15 MTS/IEEE*, pp. 1–7, IEEE, Washington, DC, USA, October 2015.

[18] F. Gustafsson and F. Gunnarsson, "Localization in sensor networks based on log range observations," in *Proceedings of the 2007 10th International Conference on Information Fusion*, pp. 1–8, Québec, Canada, July 2007.

[19] S. e. Alajlouni, M. Albakri, and P. Tarazaga, "Impact localization in dispersive waveguides based on energy-attenuation of waves with the traveled distance," *Mechanical Systems and Signal Processing*, vol. 105, pp. 361–376, 2018.

[20] D. Ginsberg and C.-P. Fritzen, "Impact identification and localization using a sample-force-dictionary—general theory and its applications to beam structures," *Structural Monitoring and Maintenance*, vol. 3, no. 3, pp. 195–214, 2016.

[21] Q. Li and Q. Lu, "Impact localization and identification under a constrained optimization scheme," *Journal of Sound and Vibration*, vol. 366, pp. 133–148, 2016.

[22] Q. Li and Q. Lu, "Force localization and reconstruction using a two-step iterative approach," *Journal of Vibration and Control*, vol. 24, no. 17, pp. 3830–3841, 2018.